Ultrasonics Sonochemistry 109 (2024) 107003

Contents lists available at ScienceDirect

Ultrasonics Sonochemistry

journal homepage: www.elsevier.com/locate/ultson

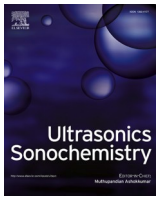

# Comparison, optimization and antioxidant activity of ultrasound-assisted natural deep eutectic solvents extraction and traditional method: A greener route for extraction of flavonoid from *Moringa oleifera* Lam. leaves

Weilong Peng [a], Xiaoguang Wang [a], Weimei Wang [a], Yaya Wang [a], Junjie Huang [a], Ruigang Zhou [a], Ruonan Bo [a,b], Mingjiang Liu [a,b], Shaojie Yin [c,*], Jingui Li [a,b,*]

[a] *School of Veterinary Medicine, Jiangsu Co-innovation Center for Prevention and Control of Important Animal Infectious Diseases and Zoonoses, Yangzhou University, Yangzhou 225009, PR China*

[b] *Joint International Research Laboratory of Agriculture and Agri-Product Safety, the Ministry of Education of China, Yangzhou University, Yangzhou, Jiangsu 225009, PR China*

[c] *Jiangsu Agri-animal Husbandry Vocational College, Taizhou, Jiangsu 225300, PR China*

ARTICLE INFO

*Keywords:*
*Moringa oleifera* Lam. leaves
Flavonoid
Natural deep eutectic solvent
Ultrasonic-assisted extraction
COSMO-RS
Antioxidant activity

ABSTRACT

To develop an environmentally sustainable and efficient extraction method for flavonoids from *Moringa oleifera Lam.* (*M. oleifera*) leaves, natural deep eutectic solvents (NADES) with ultrasound-assisted extraction was utilized in this study. After optimization of extraction parameters of NADES, including ultrasonic power, ultrasonic time, and liquid–solid ratio, the extraction yield of ultrasound-assisted NADES (UAN) composed of betaine and urea (Bet-Urea) reached 54.69 ± 0.19 mg RE/g DW, which made a 1.7-fold increase compared to traditional ultrasound-assisted traditional solvent (UATS). UPLC-Q Exactive/MS analysis revealed that *M. oleifera* leaves flavonoids (MOLF) was mainly composed of Quercetin 3-β-D-glucoside, Rutin, Kaempferol-3-O-glucoside, Vitexin and Quercetin. Furthermore, the COSMO-RS model was employed to verify the optimal compatibility of solubility and activity coefficient between Bet-Urea and the five primary flavonoids in MOLF. *In vitro* antioxidant assays verified that MOLF extracted by UAN exhibited superior antioxidant activity compared to MOLF extracted by UATS. Overall, the devised process not only augmented the extraction yield of MOLF but also effectively preserved the bioactive compounds, thus promoting the utilization of green extraction solvents in the food industry.

## 1. Introduction

*Moringa oleifera Lam.* (*M. oleifera*), originating from India, was designated as a new resource food by the Chinese Ministry of Health in 2012 [1]. *M. oleifera* holds a significant place as both a culinary ingredient and a resource in traditional Chinese medicine [2,3]. Alongside Ganoderma lucidum and American ginseng, *M. oleifera* is revered as one of the "Three Treasures of the World." The primary medicinal and edible component of *M. oleifera* is its leaf, which is abundant in protein, polysaccharides, flavonoids, and essential nutrients [4]. Among which, flavonoids are the main bioactive substances, which exhibit important pharmacological activities, including antioxidant, anti-diabetes, anti-atherosclerosis benefits [5–7]. Nevertheless, the advancement and exploitation of *M. oleifera* leaves in China remain relatively constrained. The primary challenge lies in the nascent extraction methodologies applied to *M. oleifera* leaves, coupled with the absence of suitable extraction techniques. Consequently, it is necessary to pioneer an eco-friendly and highly efficient extraction process for flavonoids derived from *M. oleifera* leaves, alongside rigorous evaluation of the extract properties.

Typically, flavonoids in plants are hydrophilic and are extracted using ultrasound-assisted traditional solvent (UATS) such as ethanol, methanol, and acetone [8,9]. Nevertheless, these organic solvents harbor numerous inherent drawbacks, including pronounced volatility, elevated toxicity, flammability, and limited biodegradability [10]. Due the adverse impacts of UATS on human health and environment, the usage of these UATS is steadily diminishing. In recent years, a novel green solvent known as natural deep eutectic solvent (NADES) has

* Corresponding authors at: College of Veterinary Medicine, Yangzhou University, Yangzhou 225009, PR China.
*E-mail addresses:* shaojie_yin@163.com (S. Yin), jgli@yzu.edu.cn (J. Li).

https://doi.org/10.1016/j.ultsonch.2024.107003
Received 29 May 2024; Received in revised form 22 July 2024; Accepted 25 July 2024
Available online 26 July 2024

emerged as a promising alternative to conventional solvents [11]. Contrasted with traditional organic solvents, NADES has garnered considerable acclaim owing to its sustainable nature, biodegradability, non-toxic properties, straightforward preparation process, and cost-effectiveness [12]. In addition, the polyphenols and flavonoids extracted by NADES show enhanced biological activities [13] and better antioxidant [14], anti-inflammatory [15], properties of α-Inhibition of glucosidase and pancreatic lipase [16]. NADES has a simple composition and is formed through hydrogen bonding interactions between hydrogen bond acceptors (HBA) and hydrogen bond donors (HBD) [17], which can be directly prepared without the need for solvent separation, and it can serve as a strategy to reduce energy consumption and auxiliary material usage during the extraction process. Ultrasonic extraction, a highly efficient, safe, and economical extraction technique, induces robust tensile force and cavitation phenomena, which can effectively rupture the plant cell walls and facilitate the release of active compounds into the extraction solvent with greater ease [18,19]. Employing ultrasonic-assisted NADES (UAN) for extracting bioactive components from plants not only significantly reduces solvent consumption, time, labor, and energy expenditure but also amplifies the precipitation of bioactive compounds through cavitation [20]. Andiri et al. reported that NADES synthesized from betaine and urea (Bet-Urea) in a ratio of 1:2 exhibits the highest rosmarinic acid content extracted from *Symphytum officinale L.* with ultrasonic assistance [15]. This particular Bet-Urea extraction demonstrates superior antioxidant and anti-inflammatory properties while exhibiting lower hepatotoxicity [15]. Therefore, UAN was utilized to extract flavonoids from *M. oleifera* leaves, and ethanol was selected as the UATS for comparison.

The purpose of this study is to: (1) identify the optimal NADES from a selection of eight representative candidates, with the goal of extracting the highest amount of flavonoids from *M. oleifera* leaves; (2) optimize the UAN extraction and UATS processes using one-way experiments and Response Surface Methodology (RSM) and compare the difference of the amount extracted by the two methods, aiming to maximize the yields of total flavonoid content (TFC) in *M. oleifera* leaves flavonoids (MOLF); (3) verify factors that significantly affect TFC using $2^k$ experimental design, and confirm the MOLF extraction efficiency of UAN using the COSMO-RS quantum chemical calculations as assistant; (4) qualitatively and quantitatively analyze the components of MOLF extracted by UAN and UATS using UPLC-Q Exactive/MS; (5) evaluate the antioxidant capacity of MOLF obtained by UAN and UATS through free radical scavenging activity, iron reducing activity and ROS reactive oxygen species assay in IPEC cells.

## 2. Materials and methods

### 2.1. Materials and reagents

*M. oleifera* leaves were purchased from Yunnan Ruziniu Biotechnology (Yunnan, China). Choline chloride, glycerol, citric acid, sucrose, urea, betaine, and ethylene glycol used for synthesizing NADES and 1,1-Dipheny-2-picrylhydrazyl (DPPH), 2,2′Azinobis-(3-ethylbenzthiazoline-6-sulphonate) (ABTS) were obtained from Macklin Biochemical Technology (Shanghai, China). Thirty-nine kinds of standard compounds such as Gallic acid, 3,4-Dihydroxybenzoic acid, and Protocatechualdehyde were purchased from Sigma Aldrich (USA). Ferric reducing antioxidant power (FRAP) test kit was obtained from Nanjing Jiancheng Biotechnology (Nanjing, China).

### 2.2. Preparation and synthesis of NADESs

In the present study, we selected different and most representative substances as HBD, glycerol and glycol as alcohols, sucrose as glycosyl, urea as amides, citric acid as organic acids. In addition, we selected choline chloride and betaine, the two most common HBA for this experiment. According to the previously reported, 8 types of NADESs were synthesized by blending the HBA and HBD in the appropriate molar ratios, continuously stirring at 1500 rpm at 80 °C until a transparent and homogeneous liquid was achieved [21,22] (Table 1). In the course of synthesis, a certain quantity of water is indispensable to diminish the viscosity of NADES. For preliminary assessment, 40 % (w/w) of water is incorporated into each NADES sample.

### 2.3. Ultrasound-assisted traditional solvent (UATS) and ultrasound-assisted NADES (UAN) extraction of MOLF

*M. oleifera* leaf powder (0.50 g) was weighted and delicately deposited into a 150 mL flask. Before extraction, NADES was meticulously diluted with water to a precise concentration, subsequently infused into the flask in accordance with a predetermined liquid–solid ratio, as shown in Fig. 1A. Ethanol was chosen as the UATS, and 70 % ethanol was mixed with powder in the flask. After that, the flask was put into a bath-type ultrasonic instrument (FB-1400DTH, Shanghai shengxi Ultrasonic Instrument Co. Ltd). Next, the extraction solution was transferred to a high-speed centrifuge (1–16 K, Sigma Aldrich) and centrifuged at 10,000 rpm for 10 min. The supernatant was collected for the subsequent experiments. Each extraction condition underwent three repetitions to ensure robustness, with the mean value being subsequently documented.

### 2.4. Determination of TFC in MOLF

TFC in MOLF were evaluated according to a previously publication (Namazi et al. 2021) [23]. In brief, a tenfold diluted extract (50 μL) was dispensed into a 96-well plate, followed by the addition of precise volumes of sodium nitrite solution (5 %, w/v) and aluminum chloride solution (10 %, w/v). Subsequently, a specific volume of NaOH solution was added to facilitate absorbance measurement at 510 nm. The standard curve equation for Rutin was $Y = 7.0657\ X + 0.053$ ($R^2 = 0.997$, $n = 5$).

### 2.5. Optimization of UATS and UAN extraction procedure

According to the previous research results [24], when the solvent was ethanol, the main factors affecting the extraction efficiency were ultrasonic power, liquid–solid ratio and ethanol concentration. So, in the present study, a single factor experiment was carried out, where only one main influencing factor was varied, other conditions were kept constant. The ultrasonic power (140, 280, 420, 560 and 700 W), liquid–solid ratio (30:1, 40:1, 50:1, 60:1 and 70:1) and ethanol concentration (50, 60, 70, 80 and 90 %) were selected to calculate the content of flavonoid compounds in the resulting MOLF. When NADES were used as extraction solvent, the molar ratio (2:1, 1:1, 1:2, 1:3 and 1:4) and water content in NADES (20, 30, 40, 50 and 60 %) were first selected to optimize. Then the influences of three significant factors through single factor experiments based on the highest extraction efficiency molar ratio and water content were evaluated, including ultrasonic power (140, 280, 420, 560 and 700 W), ultrasonic time (10, 20, 30, 40 and 50 min) and liquid–solid ratio (20:1, 30:1, 40:1, 50:1 and 60:1).

The optimization of the extraction process was conducted through

**Table 1**
Synthesis of NADES with different components and molar ratios.

| Solvent abbreviation | HBA | HBD | Molar Ratio |
|---|---|---|---|
| ChCl-EG | Choline chloride | Ethylene glycol | 1:2 |
| ChCl-Urea | Choline chloride | Urea | 2:5 |
| ChCl-Suc | Choline chloride | Sucrose | 2:1 |
| ChCl-CA | Choline chloride | Citric acid | 2:1 |
| Bet-Gly | Betaine | Glycerol | 1:1 |
| Bet-Urea | Betaine | Urea | 1:1 |
| Bet-CA | Betaine | Citric acid | 2:1 |
| Bet-Suc | Betaine | Sucrose | 2:1 |

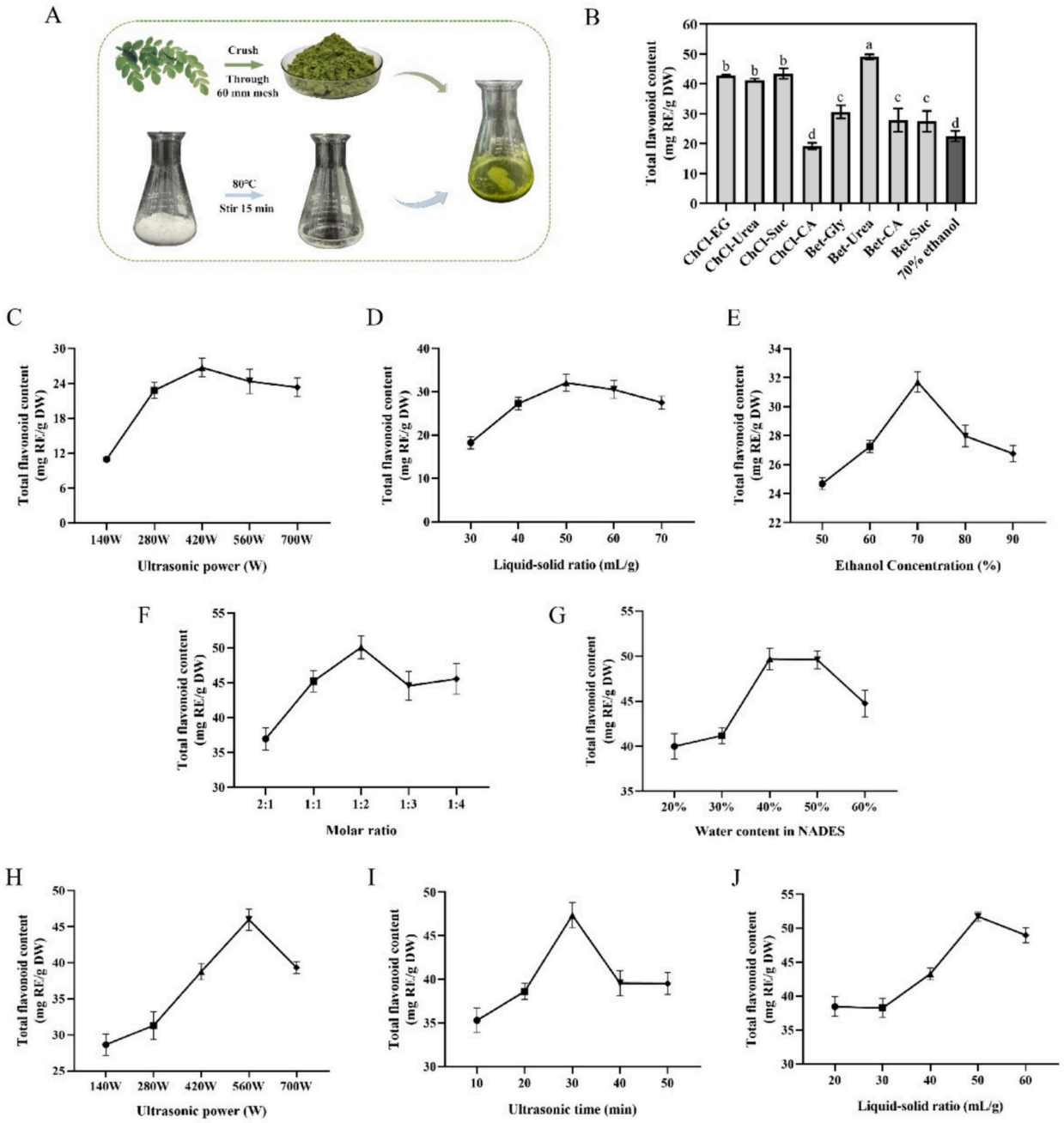


**Fig. 1.** MOLF content extracted by different NADESs and single factor experimental results. (A) Schematic diagram of NADESs preparation and MOLF extraction. (B) Extraction amount of MOLF with different NADESs. (C–E) Single factor experimental results of ultrasonic power, liquid–solid ratio and ethanol concentration for UATS. (F–G) Single factor experiment to optimize the molar ratio and water content in NADES. (H-J) Single factor experimental results of ultrasonic power, ultrasonic time and liquid–solid ratio for UAN.

RSM. A Box-Behnken Design (BBD) featuring three factors and three levels was implemented to examine the intricate relationship among the independent variables, leveraging the capabilities of Design Expert software. A total of 17 experimental sets were executed, as delineated in Tables S1, 2, with the TFC serving as the response criterion. Achieving the ideal extraction method involved maintaining variables within specified ranges to maximize yield. A validation experiment, conducted in triplicate under revised conditions adhering to optimal parameters, confirmed the effectiveness of the model.

### 2.6. *Validating statistically significant effects using $2^k$ experimental design*

A two-level analytical factorial experiment was conducted using Minitab v.21 to determine the effects of three factors (ethanol concentration [$A_1$], liquid–solid ratio [$B_1$] and ultrasound power [$C_1$]) for UATS. Certainly, when the extraction solvent is NADES, ultrasound power [$A_2$], ultrasound time [$B_2$] and liquid–solid ratio [$C_2$] were used to explore the influence of their individual or pairwise interaction on MOLF (Tables S3, 4), where TFC was the response. Criterion plots for standardized effects rely on the position of the effect point relative to the criterion line, whereas Pareto plots for standardized effects was used to assess the significance of the main or interaction effect based on the magnitude of the column compared to the other columns [25]. Response surface analysis was used to validate the key factors affecting TFC of MOLF.

### 2.7. Scanning electron microscope (SEM) observation of the microstructure of M. oleifera leaf powder

After the extraction process, the UATS and the UAN separately extracted *M. oleifera* leaf powders were placed in the 60 °C drying oven and the untreated powder was used as a control. All samples were plated with gold by ion sputtering and then observed under a SEM (S-4800 II, Hitachi Limited, Japan) with an accelerating voltage of 10.0 kV, an emission current of 1 nA, and the magnification of 3000×.

### 2.8. UPLC-Q Exactive/MS analysis

Prior to HPLC analysis, the MOLF extracted by UATS and UAN under the optimal conditions was passed through the 0.22-μm membrane filter (Millipore, USA). The sample extracts underwent analysis utilizing a UPLC–Orbitrap-MS system (UPLC: Vanquish; MS: QE). Analytical parameters were set as follows: UPLC utilized a Waters HSS T3 column (50 * 2.1 mm, 1.8 μm) at 40℃. Solvent system: water (0.1 % acetic acid) and acetonitrile (0.1 % acetic acid) with the following gradient: 90:10 V/V at 0 min, 90:10 V/V at 2.0 min, 40:60 V/V at 6.0 min, 40:60 V/V at 9.0 min, 90:10 V/V at 9.1 min, and 90:10 V/V at 12.0 min. HRMS data were obtained using a Q Exactive hybrid Q–Orbitrap mass spectrometer with a heated ESI source (Thermo Fisher Scientific), employing Fullms-ms2 acquisition methods. ESI source parameters: spray voltage −2.8 kV, sheath gas pressure 40 arb, aux gas pressure 10 arb, sweep gas pressure 0 arb, capillary temperature 320℃, and aux gas heater temperature 350℃. Data acquisition were performed on Q-Exactive using Xcalibur 4.1 (Thermo Scientific) and processed using TraceFinder™4.1 Clinical (Thermo Scientific).

### 2.9. COSMO-RS simulations

To verify the best efficiency of Bet-Urea in extracting MOLF among eight NADESs, COSMO-RS was used to simulate the interaction between NADES components and flavonoid components. The specific prediction process of this model comprised two primary steps: (1) A virtual conductor environment for the molecules were established utilizing the continuum solvation model. Density functional theory (DFT) was used for quantum chemical computations, generating a shielding charge density known as sigma (σ) on the adjacent conductor. This sigma (σ) distribution on the molecular surface was then converted into a function of surface composition, termed as the molecular surface shielding charge density distribution (σ-profile). (2) The shielding charge density σ was calculated using quantum chemistry software, yielding the COSMO file. Subsequently, based on this file the molecular energy stemming from electrostatic mismatch energy, hydrogen bonding, and van der Waals interactions were calculated using the principles of statistical thermodynamics. All 3D molecular structures were downloaded from the PUBCHEM database in SDF format and imported into Materials Studio 2020 software [26]. Solubility and activity coefficient were calculated according to the method reported by Li et al. [27].

### 2.10. Determination of antioxidant activity

#### 2.10.1. DPPH radical scavenging activity

The lyophilized sample powder were dissolved in water to a concentration of 2.0 mg/mL, then further diluted to 0.1–2 mg/mL. Vitamin C was used as the positive control. The DPPH radical scavenging capacity was determined after modification according to the method reported by Fu et al. [28]. Sample solutions (1 mL) with different concentrations and DPPH (1 mL, 0.1 mmol/L) solution were added into centrifuge tubes. The tubes were shake evenly and let stand for 30 min at 25 °C in the dark, and the absorbance A1 at a wavelength of 517 nm were measured. Ethanol (1 mL) was added into 1 mL sample with different concentrations, measured the absorbance as A2. Adding 1 mL DPPH to 1 mL absolute ethanol and measured as A0. The DPPH radical scavenging rate was calculated using the following formula: DPPH radical scavenging rate (%) = [1 − (A1-A2)/A0] × 100 %.

#### 2.10.2. $ABTS^+$ radical cation scavenging activity

The $ABTS^+$ radical scavenging rate assay followed the method described by Liu et al. [29]. Equal volumes of anhydrous ethanol and potassium persulfate aqueous solutions were mixed to prepare the $ABTS^+$ solution. The sample solution at different concentrations were mixed with the $ABTS^+$ solution and shaken, then the absorbance A1 was measured at 734 nm. The absorbance of the sample solution with deionized water was A2, and the absorbance of the $ABTS^+$ solution with deionized water was A0. The $ABTS^+$ radical scavenging rate in each sample was calculated using the following formula: $ABTS^+$ radical scavenging rate (%) = [1 − (A1-A2)/A0] × 100 %.

#### 2.10.3. Ferric reducing antioxidant power

The FRAP method was conducted following the protocol outlined by Fidrianny et al. [30] with minor adjustments, the FRAP working solution, $FeCl_3$ solution, and TPTZ hydrochloric acid were mixed in a volume ratio of 10:1:1. Subsequently, 0.2 mL of various sample concentrations were blended with the FRAP working solution (3.8 mL). The ensuing reaction took place within a water bath at 37 °C for 10 min, then the absorbance was recorded at 593 nm.

#### 2.10.4. Reactive oxygen species (ROS) detection in IPEC cells

IPEC cells were inoculated into six-well plates with cell climbing slice at $2 \times 10^5$ cells per well and incubated at 37 °C for 18 h. Subsequently, the cells were stimulated with 3 % $H_2O_2$ and given different concentrations of UAN and UATS (10 μg/mL, 50 μg/mL, 100 μg/mL, 200 μg/mL) for 4 h. Then, the cells were labelled with the DCFH-DA probe (Yeasen Biotechnology, China) and incubated at 37 °C for 40 min. Finally, the excess probe was rinsed and the fluorescence intensity was measured and photographed under a fluorescence microscope (Nikon, Japan).

### 2.11. Statistical analysis

GraphPad Prism 8 was used to analyze experimental data and draw data graphs, and statistical analysis was performed on each group of data. Statistical analysis was meticulously carried out on each data, with all experimental data presented as the mean ± standard deviation (SD). Statistical evaluation was performed through one-way Analysis of Variance (ANOVA) followed by a T test. $P<0.05$ were considered statistically significant.

## 3. Results and discussion

### 3.1. Selection of NADES for extraction of TFC from M. oleifera leaves

NADES can be used as an economical and new type of “green solvent” due to its simple preparation, no purification step, non-volatile, non-toxic and biodegradable [31]. Compared with UATS, NADES can significantly increase the extraction rate of flavonoids, and improve the existing technology of time-consuming, cumbersome operation or prolonged thermal effects leading to the decomposition and oxidation of the active ingredients. NADES efficiently dissolves cell walls due to its high hydrogen-bonding alkalinity, facilitating effective intermolecular interactions with cellulose chains [32]. Extraction efficiency primarily correlates with NADES polarity and viscosity, attributes heavily contingent upon its composition, the molar ratio of HBA to HBD, and the water content within the NADES [33]. The composition of NADESs determines the formation and stability of eutectic system. Several studies have shown that the NADES components used for the efficient extraction of polyphenolic compounds are choline chloride as the hydrogen-bond acceptor and polyols, organic acids, sugars or amides as the hydrogen-bond donor [34]. Therefore, in this study, choline chloride and

betaine from natural plants, which are cheap and easy to obtain, were selected as hydrogen-bond acceptors, and glycerol, ethylene glycol, sucrose, urea and citric acid were selected as hydrogen-bond donors. Results revealed significant differences in MOLF extraction amounts when employing various NADESs coupled with ultrasound-assisted extraction ($P < 0.05$, Fig. 1B). The efficiency of MOLF was highest when using Bet-Urea (49.04 ± 0.87 mg RE/g DW), followed by ChCl-Suc (43.47 ± 1.76 mg RE/g DW), ChCl-EG (42.78 ± 0.75 mg RE/g DW), and ChCl-Urea (41.16 ± 1.19 mg RE/g DW). Notably, the MOLF content extracted using the UATS 70 % ethanol is only 22.52 ± 1.71 mg RE/g DW, which were 45.9 % of the MOLF obtained by Bet-Urea. The viscosity and polarity of NADES significantly impact the extracted MOLF amount, high NADES viscosity can result in low conductivity and hinder compound diffusion. It is likely that the polarity of MOLF is highly similar to that of NADES, based on the principle that compounds are more likely to be dissolved in solvents with similar polarity [35]. In this study, Bet-Urea was selected as the highest extraction amount of NADES probably because the polarities of Bet-Urea and MOLF are highly similar and Bet-Urea has a suitable viscosity, which is beneficial to the precipitation of TFC. Therefore, Bet-Urea was selected as the best green solvent for subsequent experiments.

### 3.2. Single factor experiments

Regarding the traditional extracting method of MOLF, the influence of three key factors was discussed, including ultrasonic power, liquid–solid ratio, and ethanol concentration (Fig. 1C–E). During this process, all other parameters were kept constant. The single factor results showed that when the ultrasonic power is 420 W, the liquid–solid ratio is 50:1, and the ethanol concentration is 70 %, the highest MOLF content was obtained, which were 26.74 ± 1.57, 32.08 ± 2.01, and 31.71 ± 0.71 mg RE/g DW, respectively. Studies had shown that flavonoid aglycones were easily soluble in water, methanol, ethanol and other highly polar solvents. Ethanol with a concentration of 80 %–95 % is suitable for the extraction of flavonoid aglycones, while ethanol with a concentration of 70 % is suitable for the extraction of flavonoid glycosides [36], which indicating that the proportion of flavonoid glycosides in MOLF is the highest.

Based on the results in section 3.1, Bet-Urea was selected as the NADES to extract MOLF. Firstly, the influence of the molar ratio of Bet to Urea and water content in NADES on the extraction rate was investigated to select a suitable NADES system for subsequent experiments [37]. The results showed that when the molar ratio of Bet: Urea was 1:2 and the water content in NADES is 50 %, the extraction rate was the highest, which were 50.09 ± 1.64 and 49.67 ± 1.18 mg RE/g DW, respectively. Additionally, the molar ratio of HBA to HBD in NADES is crucial in the extraction process. An optimal ratio enhances interaction forces between HBA and HBD. However, excessive molar ratios can lead to increased viscosity and decreased fluidity, reducing the solubility capacity of the extract [38].The flavonoid content in this study first increased and then decreased as the increasing of Bet to Urea molar ratio (Fig. 1F). The highest MOLF yield was shown when the molar ratio of Bet and Urea was 1:2. This molar ratio was selected for subsequent experiments. When the moisture content of the NADES elevated from 20 % to 40 %, there was a progressive augmentation in extraction yield (Fig. 1G). Concurrently, the diminished system's viscosity, intensified polarity [39], expanded contact surface area with the powder, and enhanced conductivity rate catalyzes the dissolution of MOLF. At moisture contents of 40 % and 50 %, the peak extraction yields for MOLF were 49.59 ± 0.99 and 49.67 ± 1.18 mg RE/g DW, respectively. However, when the water content is greater than 50 %, the extraction amount of MOLF began to decrease. This is because that too much water content leads to a decrease in viscosity and excessive polarity, causing the hydrogen bonds between molecules to break, thereby destroying the supramolecular structure of the system [40]. The interaction between the solvent and total flavonoids is weakened, resulting in a reduction in the amount of MOLF extracted. Based on the principle of saving betaine and urea materials, we chose a 50 % of water content for the next step of the experiment.

Subsequently, we conducted the single factor experiments on ultrasound power, ultrasound time, and liquid–solid ratio. Additionally, ultrasound generates robust cavitation and mechanical vibration, causing the breakdown of plant cell tissue structure. This results in the rapid dissolution of target flavonoids in *M. oleifera* leaf cells [41]. However, the extraction effect does not always increase with increasing ultrasound power, because high ultrasonic energy may destroy the bond structure of flavonoids, resulting in a reduction in the extraction content of flavonoids [42]. Our results showed that when the ultrasonic power was lower than 560 W, the extraction rate of MOLF increased with the increasing ultrasonic power (Fig. 1H). The reason is that the increase in ultrasonic power accelerates the movement of molecules in the system, enhances the disruption of cell walls, and increases the overflow of total flavonoids. The maximum amount of MOLF extraction was 45.98 ± 1.51 at an ultrasonic power of 560 W. When ultrasound power continued to increase, the opposite trended appears. Excessive ultrasonic power may enhance cavitation, leading to the production of excessive impurities and the destruction of MOLF components, thereby reducing the extraction amount. Simultaneously, the impact of ultrasonic time on the extraction amount was also important. When the ultrasonic time increases from 10 min to 30 min, the extraction amount increased with the increase of ultrasonic time (Fig. 1I), which may be due to the cavitation effect formed by ultrasonic energy in the solvent system can induce the constantly damaged cell wall and dissolved flavonoids [43]. The extraction rate of MOLF reached the highest value at 30 min of ultrasonic time, which was 47.36 ± 1.37 mg RE/g DW. When the ultrasonic time exceeded 30 min, the extraction amount of MOLF began to decline, which may be caused by the dissolution of a large number of impurities in the system caused by the long ultrasonic time, thereby limiting dissolution of MOLF and the degradation of some flavonoids. When the liquid–solid ratio was 50:1, the maximum extraction amount of MOLF is 51.71 ± 0.67 mg RE/g DW (Fig. 1J). When the liquid–solid ratio increased from 20:1 to 50:1, the extraction amount also increased. This is attributed to the increased contact area between *M. oleifera* leaf powder and the solvent system, facilitating enhanced extraction and continuous overflow of total flavonoids [44]. When the liquid–solid ratio was more than 50:1, the extraction amount of MOLF began to decrease. Once the extraction solvent reaches a certain level, the requirement for flavonoid dissolution is essentially fulfilled. Further increasing the solvent amount yields diminishing returns in flavonoid dissolution and escalates extraction costs [41].

### 3.3. Response surface methodology

RSM was applied to optimize the MOLF extraction procedure using UAN. On the basis of single factor experiment, ethanol concentration ($A_1$, 60–80 %), liquid–solid ratio ($B_1$, 40–60 mL/g) and ultrasonic power ($C_1$, 280–560 W) were selected as variables for traditional ethanol solvent extraction, while ultrasonic power ($A_2$, 420–700 W), ultrasonic time ($B_2$, 20–40 min) and liquid–solid ratio ($C_2$, 40–60 mL/g) were selected as variables for UAN extraction method, and MOLF extraction amount was selected as response value. The design and results of RSM were shown in Tables S1, 2, while the ANOVA results were provided in Table 2. The relationship between the extraction amount of MOLF using UATS and the variables $A_1$, $B_1$, and $C_1$ could be described by the following equation (1): $Y_1 = 32.26 + 0.3428A_1 + 0.4044B_1 + 0.9016C_1 - 0.1233A_1B_1 + 0.5183A_1C_1 - 0.1600B_1C_1 - 1.78A_1^2 - 1.73B_1^2 - 2.04C_1^2$. While the relationship between the extraction amount of MOLF using UAN and variables A2, B2, and C2 was represented by the following equation (2): $Y_2 = 54.57 + 1.09A_2 + 1.09B_2 + 1.72C_2 + 0.3053A_2B_2 + 0.2730A_2C_2 - 0.1078B_2C_2$—$3.30A_2^2 - 3.71B_2^2 - 4.38C_2^2$. Table 2 shows a low $P$ value ($P<0.0001$) and high F value ($F_{UATS}=44.29$, $F_{UAN}=3005.02$), indicating the statistical significance of the regression

**Table 2**
Analysis of variance results of RSM.

| Source | Sum of Squares | | df | Mean Square | | F-value | | p-value | |
|---|---|---|---|---|---|---|---|---|---|
| | UATS | UAN | | UATS | UAN | UATS | UAN | UATS | UAN |
| Model | 58.57/249.29 | | 9 | 6.51/27.7 | | 44.29/3005.02 | | <0.0001 | |
| $A_1/A_2$ | 0.9398/9.46 | | 1 | 0.9398/9.46 | | 6.40/1026.22 | | 0.0393/<0.0001 | |
| $B_1/B_2$ | 1.31/9.51 | | 1 | 1.31/9.51 | | 8.90/1032.13 | | 0.0204/<0.0001 | |
| $C_1/C_2$ | 6.50/23.79 | | 1 | 6.50/23.79 | | 44.26/2581.49 | | 0.0003/<0.0001 | |
| $A_1B_1/A_2B_2$ | 0.0608/0.3727 | | 1 | 0.0608/0.3727 | | 0.4136/40.44 | | 0.5407/0.0004 | |
| $A_1C_1/A_2C_2$ | 1.07/0.2981 | | 1 | 1.07/0.2981 | | 7.31/32.34 | | 0.0305/0.0007 | |
| $B_1C_1/B_2C_2$ | 0.1024/0.0464 | | 1 | 0.1024/0.0464 | | 0.6969/5.04 | | 0.4314/0.0597 | |
| $A_12/A_2^2$ | 13.41/45.88 | | 1 | 13.41/45.88 | | 91.24/4977.59 | | <0.0001 | |
| $B_12/B_2^2$ | 12.56/57.95 | | 1 | 12.56/57.95 | | 85.48/6286.63 | | <0.0001 | |
| $C_12/C_2^2$ | 17.53/80.68 | | 1 | 17.53/80.68 | | 119.33/8753.48 | | <0.0001 | |
| Residual | 1.03/0.0645 | | 7 | 0.1469/0.0092 | | | | | |
| Lack of Fit | 0.8423/0.0347 | | 3 | 0.2808/0.0116 | | 6.03/1.55 | | 0.0576/0.3326 | |
| Pure Error | 0.1862/0.0298 | | 4 | 0.0465/0.0075 | | | | | |
| Cor Total | 59.59/249.35 | | 16 | | | | | | |
| $R^2$ | | | | | | 0.9827/0.9997 | | | |
| Adjusted $R^2$ | | | | | | 0.9606/0.9994 | | | |

model. The lack of fit term was insignificant ($P$>0.05), confirming the model validity. The coefficient of determination ($R^2_{UATS}$ = 0.9827, $R^2_{UAN}$ = 0.9997) and adjusted coefficient of determination (Adjusted $R^2_{UATS}$ = 0.9606, Adjusted $R^2_{UAN}$ = 0.9994) suggest that the regression model is suitable and can predict subsequent results accurately. According to the F value, the order of the factors that affect the extraction amount of MOLF using UATS extraction methods was: ethanol concentration ($A_1$) > ultrasonic power ($C_1$) > liquid–solid ratio ($B_1$), and the factors that affect the extraction amount of MOLF using UAN extraction method was: liquid–solid ratio ($C_2$) > ultrasonic time ($B_2$) > ultrasonic power ($A_2$).

To clarify the interaction of the three variables on the MOLF, 3D response surfaces were applied (Fig. 2). The response surface could intuitively reflect whether the interaction between the two factors was obvious. The greater the inclination of the surface in the three-dimensional graph, the darker the color in the two-dimensional graph, the more approximate the ellipse of the graph, and the closer the distance between contour lines, indicates that the interaction between the two factors is more obvious, otherwise the interaction was not significant [45]. In Fig. 2B, the curve of $A_1C_1$ interaction showed a good inclination, and the contour lines were oval and dense, indicating that the interaction of ethanol concentration and ultrasonic power had a significant impact on the extraction amount of MOLF. The RSM had a steep slope, and the contour line was oval, indicating that C2 and A2 and the interaction of B2 and C2 had a significant impact on the amount of MOLF extraction (Fig. 2G, I). The predicted optimal parameters for MOLF extraction by UATS were: 72.3 % ethanol concentration, 51.3 mL/g liquid–solid ratio, and 434 W ultrasonic power, resulting in a predicted MOLF content of 32.4 mg RE/g DW. Meanwhile, optimal extraction conditions for MOLF by UAN were: 579 W of ultrasonic power, 33 min ultrasonic time, and 51.6 mL/g liquid–solid ratio, with a predicted MOLF content of 54.82 mg RE/g DW. In order to operate easily, the verification experiments of UATS extraction were performed under 72 % of ethanol concentration, 51 mL/g of liquid–solid ratio, and 420 W of ultrasonic power; the verification experiments of UAN extraction were performed under 560 W of ultrasonic power, 33 min of ultrasonic time and 51 mL/g of liquid–solid ratio. The experimental values determined were 32.06 ± 0.24 mg RE/g DW and 54.69 ± 0.19 mg RE/g DW in UATS and UAN, respectively, which accurately matched our predicted values with a low error.

### 3.4. A two-level factorial experiment for verification of factors significantly affecting MOLF

In this study, the experimental model provided by the two-level factorial experiment (Tables S3, 4) was used to generate normality and pareto plots (Fig. 3A–D) in order to validate the main and interaction effects of the factors on the amount of MOLF extracted. The standardized Pareto charts were visualized in this study (Fig. 3A and C). Each bar represents an effect, arranged from most pronounced to least, with its length correlating to its standardized effect. A vertical line at the 0.05 critical value marks the threshold for statistical significance. Bars extending to the right of this line indicate effects achieving statistical significance at the 5 % level [46]. When using UATS to extract MOLF (Fig. 3A), the ethanol concentration, ultrasound power, and their interaction had a positive influence on the response variable, meaning that changes in these variables will lead to changes in the amount of MOLF extracted. Similar to the partial response surface experiment in the previous section, with the exception of the varied effect of the liquid–solid ratio on the extraction amount. The divergence may be attributed to the nearly identical extraction quantities of MOLF observed at liquid–solid ratios of 40:1 and 60:1. This assertion found validation in the outcomes of the single-factor experiments delineated in the 3.2 section. When using UAN to extract MOLF (Fig. 3C, D), the impact on the extraction amount in descending order was liquid–solid ratio, ultrasound time, and ultrasound power. Meanwhile, the interaction between liquid–solid ratio and ultrasonic time, liquid–solid ratio and ultrasonic power also had a significant effect on the extraction amount. This result was consistent with the response surface result, and it can be seen that the liquid–solid ratio played the most important role in the extraction of MOLF by UAN. However, the interaction plots clearly showed that the extraction of the MOLF was not dependent on a single factor but rather on a combination of influences of different single factors and their interactions (Fig. 3B and D).

### 3.5. Microstructure of the M. oleifera leaf powder

The *M. oleifera* leaf powder treated with different extraction methods was examined using SEM. The surface of untreated powder appeared smooth, with well-preserved cell structure and intact cell walls (Fig. 4B). In contrast, powder treated with UATS exhibited rough surfaces and visible cracks, though the fundamental cellular structure remained observable (Fig. 4D). This phenomenon arises from the ultrasonic-assisted 70 % ethanol extraction process, wherein ultrasonic waved facilitates penetration, enabling the solvent to breach the cellular membrane, resulting in its disintegration. Furthermore, the cavitation bubbles engendered during the ultrasonic procedure further exacerbate the disruption of the cell wall [47,48]. The morphological characteristics of the powder subsequent to ultrasonic assisted Bet-Urea extraction were also illustrated (Fig. 4F). The botanical structure experienced profound degradation, with the cellular framework being entirely compromised, manifesting numerous cavities and juxtaposed fracture

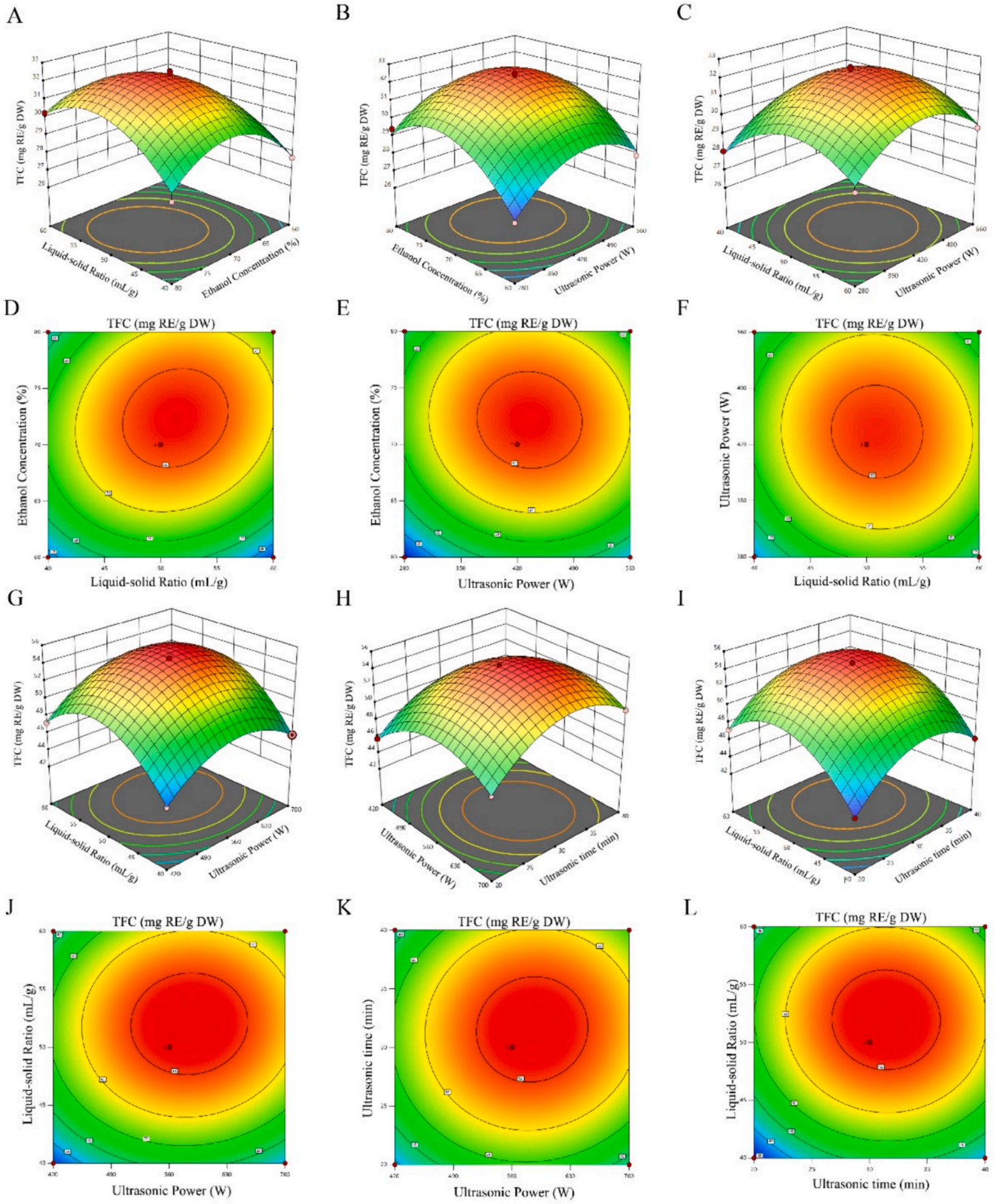


**Fig. 2.** Three-dimensional (3D) response surface of the RSM design for MOLF. (A, D) Effects of liquid–solid ratio and ethanol concentration on the yield of MOLF extracted by UATS. (B, E) Effects of ultrasonic power and ethanol concentration on the yield of MOLF extracted by UATS. (C, F) Effects of ultrasonic power and liquid–solid ratio on the yield of MOLF extracted by UATS. (G, J) Effects of ultrasonic power and liquid–solid ratio on the yield of MOLF extracted by UAN. (H, K) Effect of ultrasonic power and ultrasonic time on yield of MOLF by UAN. (I, L) Effects of liquid–solid ratio and ultrasonic time on the yield of MOLF extracted by UAN.

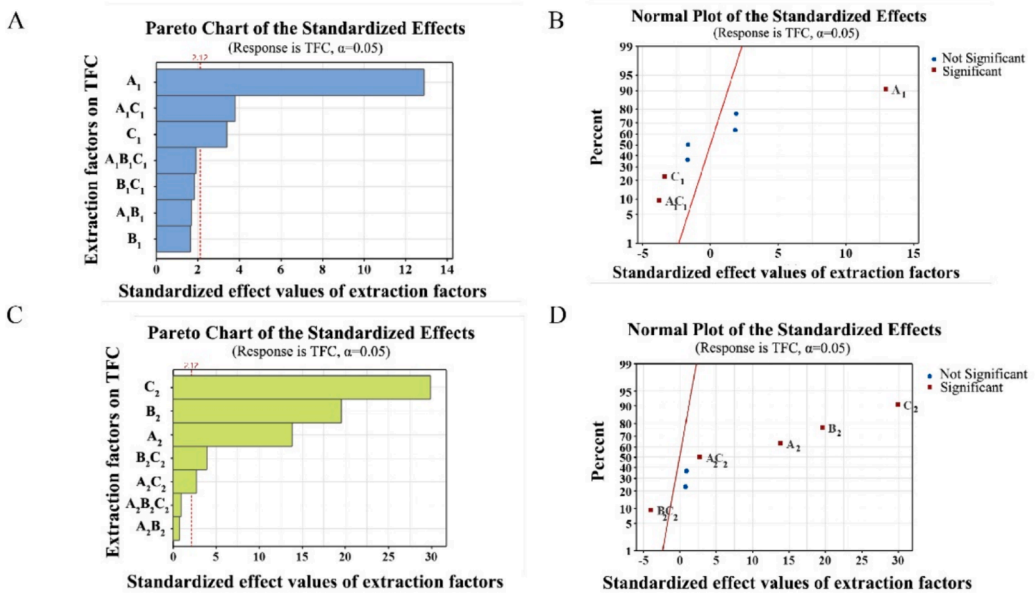


**Fig. 3.** The pareto chart (A, C) and the normal plot (B, D) obtained from two-level factorial experiment showing the significance of the primary and interaction effects: Factor $A_1$, $B_1$, $C_1$, ethanol concentration, liquid–solid ratio and ultrasonic power of UATS; Factor $A_2$, $B_2$, $C_2$, ultrasonic power, ultrasonic time and liquid–solid ratio of UAN.

planes, thereby augmenting the surface area. This heightened disruption could be attributed to the synergistic interplay between ultrasonic waves and the NADES solvent [49], expediting cellular disintegration and facilitating the solubilization of flavonoids. This indicated that the penetration and invasion ability of using NADES solvent on *M. oleifera* leaves leaf powder was better than that of 70 % ethanol.

### 3.6. Qualitative and quantitative analysis of MOLF by UPLC-Q Exactive/MS

A total of 39 kinds of polyphenol standards (including flavonoids) such as gallic acid, 3,4-dihydroxybenzoic acid and Protocatechualdehyde were selected for qualitative and quantitative analysis of MOLF components extracted by UATS and UAN (Table 3). The UPLC-Q Exactive/MS data were processed using TraceFinder software for baseline filtering, peak matching and other preprocessing steps [50]. The Total Ion Flow Chromatography (TIC) was a continuous plot obtained by adding up the intensities of all ions in the mass spectrum at each time point (Fig. 4A). The horizontal axis depicts retention time, while the vertical axis represents ion flow intensity for ion detection. The TIC peak patterns of extracting MOLF using UATS were disorderly (Fig. 4C), which may be influenced by many non-target substances. Nevertheless, the peak spectrum of MOLF extracted by UAN was clear and obvious, and the TIC of MOLF extracted by UAN was different from that extracted by UATS, which suggested that the components of MOLF extracted by the two methods may be different.

Compared with UATS extraction methods, 3,4-Dihydroxybenzoic acid, Catechin, and (+)-Dihydroxyquercetin were detected in MOLF extracted with UAN, all of which belong to flavonoid compounds. Meanwhile, Daidzein and Isoliquiritigenin were also detected, both of which belong to isoflavones. This proved that using UAN was more conducive to extracting a more diverse range of flavonoid compounds. The components with the highest MOLF content obtained by the two extraction methods were basically similar, ranked from high to low as Quercetin 3-β-D-glucoside, Rutin, Kaempferol-3-O-glucoside, Vitexin, Quercetin, which is consistent with the report by Chigurupati et al. [51]. The above results indicated that NADES is a good solvent for extracting natural products, and compared to UATS, multiple extraction products could be obtained. Compared with previous reports, the types and quantities of extraction products from different NADES varied, and the principle of extraction mechanism was more important in future research.

### 3.7. COSMO-RS model for verifying the solubility of flavonoids

In this study, COSMO-RS model was used to study the affinity between flavonoids and NADES, and reflected the charge in the molecular configuration. COSMO-RS model verified the solubility of eight different NADES for flavonoids, and explained why Bet-Urea has the highest extraction efficiency for MOLF [52]. A geometric model of five major flavonoids (Quercetin 3-β-D-glucoside, Rutin, Kaempferol-3-O-glucoside, Vitexin, Quercetin) in MOLF, Bet-Urea was constructed (Fig. 5B).Here, the green segment signifies the non-polar "neutral" moiety of the molecule, the red segment denotes the negatively charged "hydrogen receptor" region, and the blue segment represents the positively charged "hydrogen donor" region [53]. The sigma distribution across the five flavonoids ranged from −0.0084 e/Å$^2$ to 0.0084 e/Å$^2$, indicating that they were non-polar. Furthermore, the σ-profile extended into the positive domain (σ > 0.0084 e/Å$^2$), implying that these flavonoids were inclined to function as HBA. This suggests that HBD in NADES exert a pronounced influence on the extraction efficiency of flavonoids from MOLF. Although NADES is composed of HBA and HBD, its ability to dissolve flavonoids in MOLF could not be determined by the combination of HBA and HBD alone σ-profile to determine. COSMO-RS model should be used to further calculate the solubility and activity coefficients of five flavonoids in NADES. The solubility and activity coefficients of flavonoids in five MOLF in NADES with different molar ratios were calculated at t = 298.15 K (Fig. 5C, D). The activity coefficient of a substance at infinite dilution ($\gamma^{\infty}$) serves as an evaluation parameter to determine the most effective NADES for flavonoid extraction. The solubility of compounds in solvents is inversely proportional to their activity coefficients in the system [54]. The results showed that the solubility order of five flavonoids in MOLF in different NADES was Bet-Urea (1:1) > Bet-Gly (1:1) > Bet-CA (2:1) > Bet-Suc (2:1) > ChCl-EG (1:2) > ChCl-Urea (2:5) > ChCl-Suc (2:1) > ChCl −CA (2:1). The σ-profile, activity coefficient and solubility determined through the COSMO-RS model elucidated that Bet-Urea exhibited the best extraction effect on MOLF. However, the results showed that the

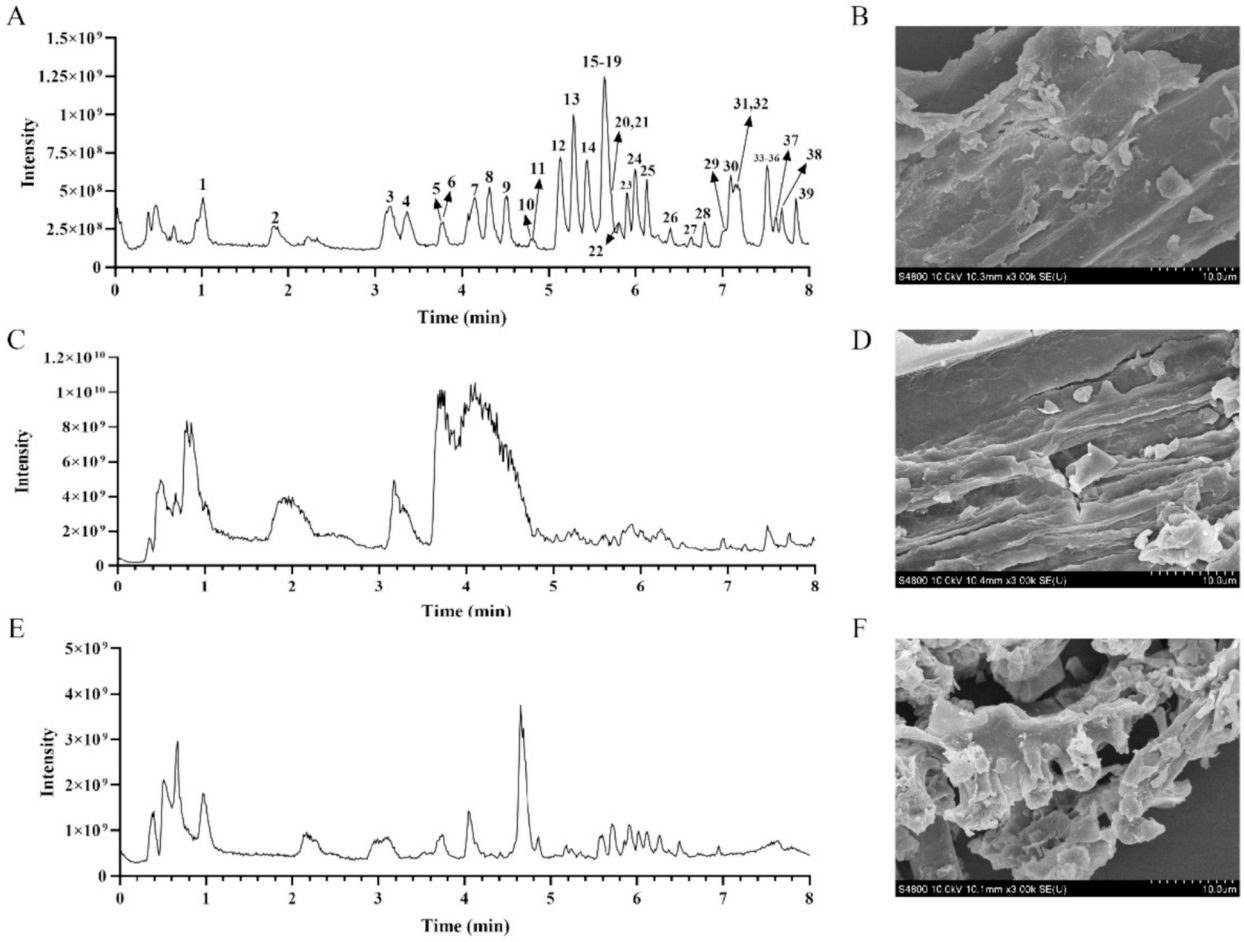


**Fig. 4.** Total Ion Flow Chromatography of phenolic compositions in the mixed standard solution (A), UATS (C), and UAN (E); SEM of *M. oleifera* powder before extraction (B), after extraction by UATS (D), and after extraction by UAN (F). 1, Gallic acid; 2, 3,4-Dihydroxybenzoic acid; 3, Protocatechualdehyde; 4, 4-Hydroxybenzoic acid; 5, Phthalic acid; 6, Catechin; 7, Vanillic acid; 8, Caffeic acid; 9, Syringic acid; 10, Epicatechin; 11, Dihydromyricetin; 12, Vanillin; 13, p-Hydroxycinnamic Acid; 14, Syringaldehyde; 15, Rutin; 16, Vitexin; 17, Trans-Ferulic acid; 18, Sinapic Acid; 19, Salicylic acid; 20, Luteoloside; 21, Quercetin 3-β-D-glucoside; 22, (+)-Dihydroquercetin; 23, Genistin; 24, Benzoic acid; 25, Kaempferol-3-O-glucoside; 26, (+)-Dihydrokaempferol; 27, Resveratrol; 28, Daidzein; 29, Luteolin; 30, Quercetin; 31, Hydrocinnamic acid; 32, Trans-Cinnamic acid; 33, Naringenin Chalcone; 34, Phloretin; 35, Naringenin; 36, Apigenin; 37, Kaempferol; 38, Isorhamnetin; 39, Isoliquiritigenin.

content of MOLF extracted by Bet-Gly was high. Nonetheless, during practical application, deviations from the predicted Bet-Gly extraction results by the model occur due to the intricate interplay of physical and chemical properties of plant raw materials, target compounds, and varying solvents.

### 3.8. *In vitro antioxidant activities*

#### 3.8.1. *DPPH scavenging abilities of MOLF extracted from UAN and UATS*

DPPH is extensively utilized for the quantitative assessment of the antioxidant capacity of biological samples, phenolic substances and foods [55]. The scavenging capacity of MOLF extracted by UAN was higher than that extracted by UATS in the range of 0.2–2.0 mg/mL (Fig. 6A). When the concentration was 0.8 mg/mL, the scavenging ability of UAN group reached the peak, which was 77.56 ± 1.82 %, while the clearance ability of UATS group was only 66.63 ± 3.15 %. However, the VC group had already reached its peak at 0.1 mg/mL, which was 87.91 ± 0.19 %. The $IC_{50}$ of the UAN group was 0.21 mg/mL, while the $IC_{50}$ of the UATS group was 0.47 mg/mL. At a concentration of 2 mg/mL, the clearance ability of these two groups was similar.

#### 3.8.2. *$ABTS^{+}$ scavenging abilities of MOLF extracted from UAN and UATS*

ABTS free radical scavenging ability detection method is a commonly used antioxidant activity evaluation method [56]. This method is mainly based on the reduction of ABTS free radicals to alcohols under visible light, and at the same time generates green $ABTS^{+}$ ions. Our study indicated that the free radical scavenging cationic activity of $ABTS^{+}$ was concentration dependent of sample concentration, and reached the maximum value at 1.2, 1.6 and 0.5 mg/mL for UAN, UATS and VC groups, respectively (Fig. 6B). The $IC_{50}$ of UAN and UATS groups were 0.32 and 0.45 mg/mL, respectively, which indicated that the MOLF extracted by UAN had better free radical scavenging ability than that extracted by UATS in the low concentration range.

#### 3.8.3. *Ferric reducing antioxidant power*

In the oxidation–reduction process, the reduction potential of transition metal ions is very important for the pre oxidation reaction. FRAP method can be used to determine the reducing activity of $Fe^{3+}$ in single electron transfer reaction [57]. The MOLF exhibited notable iron reduction capability, aligning with the experimental outcomes of DPPH and ATBS (Fig. 6C). These findings suggested that flavonoids possessing robust antioxidant properties constitute a significant portion of the constituents within UAN. However, it is plausible that the antioxidant activity of MOLF extracted via UATS are comparatively lower than that of the UAN group within the low concentration range, potentially attributed to an excess of non-flavonoid impurities or substances lacking

**Table 3**
The phenolic compounds identified in the *M. oleifera* leaves extract using UPLC-Q Exactive/MS.

| Peak | Phenolic compounds | RT (min) | Curve Equation | Ion mode | Expected Mass (*m/z*) | Detect Mass (*m/z*) | Molecular | Quantitative results (ng/100 mg) | |
|---|---|---|---|---|---|---|---|---|---|
| | | | | | | | | UATS | UAN |
| 1 | Gallic acid | 0.97 | Y = 1.263e5X; R^2: 0.9988 | $[M-H]^-$ | 169.01425 | 169.01442 | $C_9H_8O_4$ | 126.28 | 112.61 |
| 2 | 3,4-Dihydroxybenzoic acid | 1.87 | Y = 2.105e5X; R^2: 0.9991 | $[M-H]^-$ | 153.01933 | 153.01939 | $C_7H_8O_4$ | 0 | 94.8764 |
| 3 | Protocatechualdehyde | 3.15 | Y = 4.92e5X; R^2: 0.9972 | $[M-H]^-$ | 137.02442 | 137.02455 | $C_7H_6O_3$ | 189.6687 | 198.1469 |
| 4 | 4-Hydroxybenzoic acid | 3.37 | Y = 4.13e5X; R^2: 0.9986 | $[M-H]^-$ | 137.02442 | 137.02453 | $C_7H_6O_3$ | 564.3413 | 48.8663 |
| 5 | Phthalic acid | 3.55 | Y = 1.862e5X; R^2: 0.9971 | $[M-H]^-$ | 165.01933 | 165.01951 | $C_8H_6O_4$ | 55.0559 | 12.5370 |
| 6 | Catechin | 3.96 | Y = 2.129e5X; R^2: 0.9987 | $[M-H]^-$ | 289.07176 | 289.07180 | $C_{15}H_{14}O_6$ | 0 | 6.5603 |
| 7 | Vanillic acid | 4.15 | Y = 2.594e5X; R^2: 0.9967 | $[M-H]^-$ | 167.03498 | 167.03495 | $C_8H_8O_4$ | 65.3074 | 69.0689 |
| 8 | Caffeic acid | 4.32 | Y = 3.437e5X; R^2: 0.9984 | $[M-H]^-$ | 179.03498 | 179.03495 | $C_9H_8O_4$ | 95.6597 | 114.9990 |
| 9 | Syringic acid | 4.51 | Y = 2.286e5X; R^2: 0.9959 | $[M-H]^-$ | 197.04555 | 197.04525 | $C_9H_{10}O_5$ | 29.4810 | 5.8379 |
| 10 | Epicatechin | 4.8 | Y = 2.839e5X; R^2: 0.9991 | $[M-H]^-$ | 289.07176 | 289.07180 | $C_{15}H_{14}O_6$ | 27.3483 | 12.2006 |
| 11 | Dihydromyricetin | 4.84 | Y = 1.681e5X; R^2: 0.9991 | $[M-H]^-$ | 319.04594 | 319.04650 | $C_{15}H_{12}O_8$ | 10.1517 | 0 |
| 12 | Vanillin | 5.13 | Y = 4.865e5X; R^2: 0.9980 | $[M-H]^-$ | 151.04007 | 151.04011 | $C_8H_8O_3$ | 82.0749 | 12.3972 |
| 13 | p-Hydroxycinnamic Acid | 5.29 | Y = 5.512e5X; R^2: 0.9967 | $[M-H]^-$ | 163.04007 | 163.04016 | $C_9H_8O_3$ | 140.2255 | 140.3931 |
| 14 | Syringaldehyde | 5.44 | Y = 4.498e5X; R^2: 0.9982 | $[M-H]^-$ | 181.05063 | 181.05082 | $C_9H_{10}O_4$ | 46.3723 | 2.7447 |
| 15 | Rutin | 5.57 | Y = 1.857e5X; R^2: 0.9998 | $[M-H]^-$ | 609.14611 | 609.14721 | $C_{27}H_{30}O_{16}$ | 8021.0908 | 5279.7812 |
| 16 | Vitexin | 5.59 | Y = 3.239e5X; R^2: 0.9995 | $[M-H]^-$ | 431.09837 | 431.09902 | $C_{21}H_{20}O_{10}$ | 3321.3972 | 2763.9433 |
| 17 | Trans-Ferulic acid | 5.64 | Y = 3.356e5X; R^2: 0.9949 | $[M-H]^-$ | 193.05063 | 193.05062 | $C_{10}H_{10}O_4$ | 71.5878 | 5.0263 |
| 18 | Sinapic Acid | 5.68 | Y = 2.42e5X; R^2: 0.9911 | $[M-H]^-$ | 223.0612 | 223.06108 | $C_{11}H_{12}O_5$ | 10.9371 | 1.7345 |
| 19 | Salicylic acid | 5.69 | Y = 6.365e5X; R^2: 0.9994 | $[M-H]^-$ | 137.02442 | 137.02450 | $C_7H_6O_3$ | 489.9950 | 10.8328 |
| 20 | Luteoloside | 5.73 | Y = 1.722e5X; R^2: 0.9983 | $[M-H]^-$ | 447.09328 | 447.0936 | $C_{21}H_{20}O_{11}$ | 5.7844 | 1.2725 |
| 21 | Quercetin 3-β-D-glucoside | 5.72 | Y = 2.5e5X; R^2: 0.9986 | $[M-H]^-$ | 463.0882 | 463.08837 | $C_{21}H_{20}O_{12}$ | 11678.9481 | 10123.7660 |
| 22 | (+)-Dihydroquercetin | 5.81 | Y = 3.025e5X; R^2: 0.9986 | $[M-H]^-$ | 303.05103 | 303.05087 | $C_{15}H_{12}O_7$ | 0 | 0.7548 |
| 23 | Genistin | 5.81 | Y = 3.016e4X; R^2: 0.9992 | $[M-H]^-$ | 431.09837 | 431.09872 | $C_{21}H_{20}O_{10}$ | 169.2535 | 469.7720 |
| 24 | Benzoic acid | 6 | Y = 1.553e5X; R^2: 0.9981 | $[M-H]^-$ | 121.0295 | 121.02959 | $C_7H_6O_2$ | 526.1856 | 43.1915 |
| 25 | Kaempferol-3-O-glucoside | 6.05 | Y = 1.968e5X; R^2: 0.9999 | $[M-H]^-$ | 447.09328 | 447.09384 | $C_{21}H_{20}O_{11}$ | 5325.7156 | 5519.1712 |
| 26 | (+)-Dihydrokaempferol | 6.41 | Y = 6.226e5X; R^2: 0.9993 | $[M-H]^-$ | 287.05611 | 287.05599 | $C_{15}H_{12}O_6$ | 4.7764 | 0.7477 |
| 27 | Resveratrol | 6.65 | Y = 3.53e5X; R^2: 0.9997 | $[M-H]^-$ | 227.07137 | 227.07122 | $C_{14}H_{12}O_3$ | 0 | 0 |
| 28 | Daidzein | 6.8 | Y = 1.008e6X; R^2: 0.9981 | $[M-H]^-$ | 253.05063 | 253.05050 | $C_{15}H_{10}O_4$ | 0 | 0.0284 |
| 29 | Luteolin | 7.01 | Y = 7.059e5X; R^2: 0.9996 | $[M-H]^-$ | 285.04046 | 285.04034 | $C_{15}H_{10}O_6$ | 6.1846 | 1.3495 |
| 30 | Quercetin | 7.05 | Y = 4.001e5X; R^2: 0.9996 | $[M-H]^-$ | 301.03538 | 301.03521 | $C_{15}H_{10}O_7$ | 936.9820 | 136.9240 |
| 31 | Hydrocinnamic acid | 7.1 | Y = 2.672e5X; R^2: 0.9967 | $[M-H]^-$ | 149.0608 | 149.06085 | $C_9H_{10}O_2$ | 9.3104 | 2.8835 |
| 32 | Trans-Cinnamic acid | 7.19 | Y = 2.507e5X; R^2: 0.9978 | $[M-H]^-$ | 147.04515 | 147.04537 | $C_9H_8O_2$ | 114.7984 | 15.2503 |
| 33 | Naringenin Chalcone | 7.49 | Y = 2.167e5X; R^2: 0.9982 | $[M-H]^-$ | 271.0612 | 271.06103 | $C_{15}H_{12}O_5$ | 0 | 0 |
| 34 | Phloretin | 7.5 | Y = 1.307e6X; R^2: 0.9990 | $[M-H]^-$ | 273.07685 | 273.07641 | $C_{15}H_{14}O_5$ | 0.1717 | 0.0466 |
| 35 | Naringenin | 7.53 | Y = 1.094e6X; R^2: 0.9973 | $[M-H]^-$ | 271.0612 | 271.06167 | $C_{27}H_{32}O_{14}$ | 5.5369 | 1.8217 |
| 36 | Apigenin | 7.53 | Y = 1.377e6X; R^2: 0.9993 | $[M-H]^-$ | 269.04555 | 269.04559 | $C_{15}H_{10}O_5$ | 2.0768 | 0.3556 |

(*continued on next page*)

**Table 3** (*continued*)

| Peak | Phenolic compounds | RT (min) | Curve Equation | Ion mode | Expected Mass (*m/z*) | Detect Mass (*m/z*) | Molecular | Quantitative results (ng/100 mg) | |
|---|---|---|---|---|---|---|---|---|---|
| | | | | | | | | UATS | UAN |
| 37 | Kaempferol | 7.62 | Y = 8.581e5X; R^2: 0.9991 | $[M-H]^-$ | 285.04046 | 285.04040 | $C_{15}H_{10}O_6$ | 89.6168 | 20.4347 |
| 38 | Isorhamnetin | 7.69 | Y = 9.187e5X; R^2: 0.9991 | $[M-H]^-$ | 315.05103 | 315.05108 | $C_{16}H_{12}O_7$ | 91.1687 | 7.4387 |
| 39 | Isoliquiritigenin | 7.85 | Y = 1.63e6X; R^2: 0.9985 | $[M-H]^-$ | 255.06628 | 255.06616 | $C_{15}H_{12}O_4$ | 0 | 0.1033 |

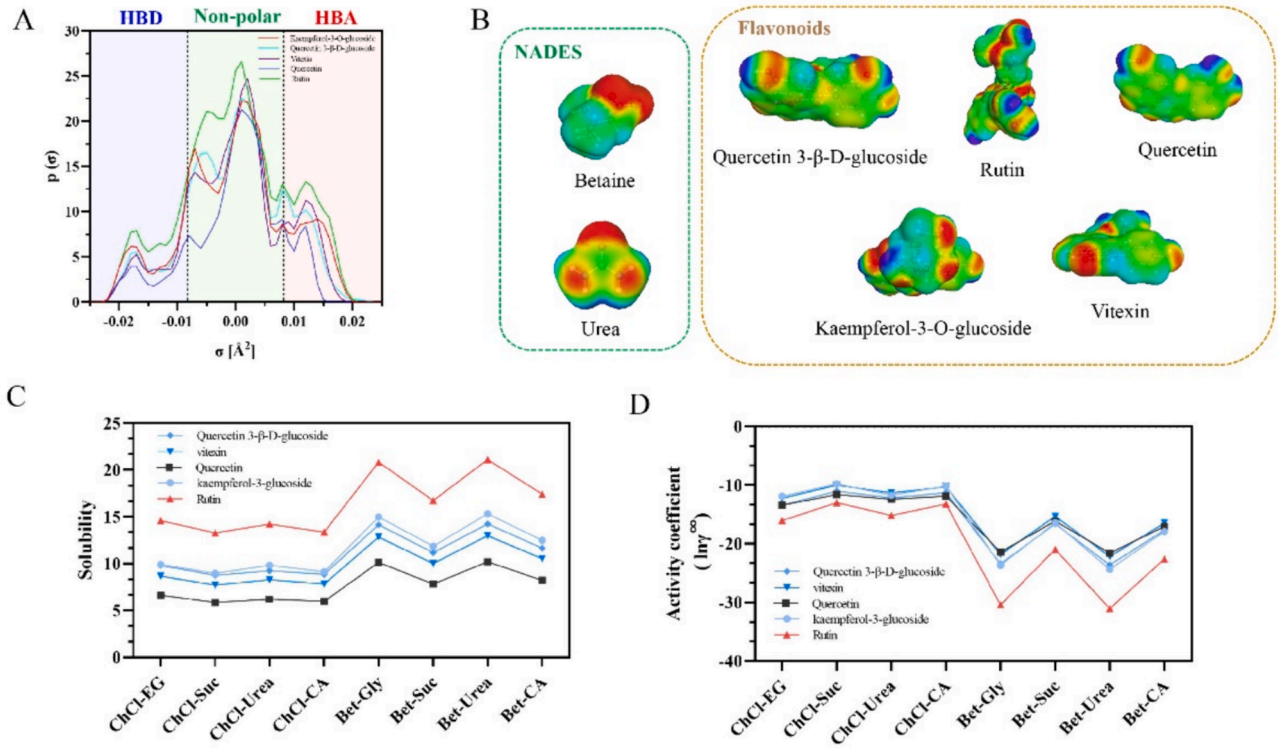


**Fig. 5.** Sigma-profiles of five main flavonoids in MOLF (A) and geometric optimization of molecular structures of betaine, urea and flavonoids (B); Solubility (C) and activity coefficients (D) of five main flavonoids in MOLF.

antioxidant activity. Feng et al. found that the antioxidant activity of *Camellia oleifera* polyphenols extracted using DES composed of choline chloride and fructose is significantly higher than that extracted using 80 % ethanol [26]. It was worth noting that at 1.6 mg/mL, the antioxidant activity of UAN group had been similar to that of VC group. Until 2.0 mg/mL, the antioxidant activities of the three groups were basically the same, which indicated that MOLF shows good antioxidant activity *in vitro*.

### *3.8.4. Protective effect of MOLF on $H_2O_2$ induced oxidative damage in IPEC cells*

In order to verify the antioxidant effect of MOLF obtained by different extraction methods *in vitro*, the $H_2O_2$ induced oxidative stress model of IPEC cells was established. The ROS level in cells was quantified by measuring the fluorescence intensity of probe DCFH-DA. The results showed that 3 % $H_2O_2$ could significantly increase the intensity of intracellular oxidative stress, while 10–200 μg/mL UAN and VC could significantly reduce the oxidative degree of IPEC cells, and 50–200 μg/mL UATS exhibited a similar effect (Fig. 6D). The antioxidant capacity of the three treatments exhibited a concentration-dependent pattern. Notably, at equivalent concentrations, the UAN group demonstrated a superior antioxidant capacity compared to the UATS group. This suggested that the MOLF extracted by UAN can effectively diminish the fluorescence intensity of ROS in IPEC cells, and may play a role in protecting IPEC cells from free radical damage by reducing the amount of ROS.

## 4. Conclusions

In this study, we compared the extraction of flavonoids from *M. oleifera* leaves using NADES and traditional solvent 70 % ethanol, and investigated their extraction, composition, and biological activity. To accomplish this objective, we meticulously selected the optimal NADES with betaine as the HBA and urea as the HBD, maintaining a molar ratio of 1:2 and a water content of 50 % from eight representative NADES. The extraction yield was optimized through single-factor experiments and RSM. Under the optimal circumstances, the content of MOLF extracted by UAN was 54.69 ± 0.19 mg RE/g DW, whereas that extracted by UATS amounted to only 32.06 ± 0.24 mg RE/g DW, representing a 1.7-fold increase in extraction yield. Subsequently, UPLC-Q Exactive/MS was used to compare the MOLF components extracted by the two methods, which will facilitate further identification of the components. Furthermore, based on the COSMO-RS model, the five principal flavonoids in MOLF were validated to exhibit the highest solubility in the NADES

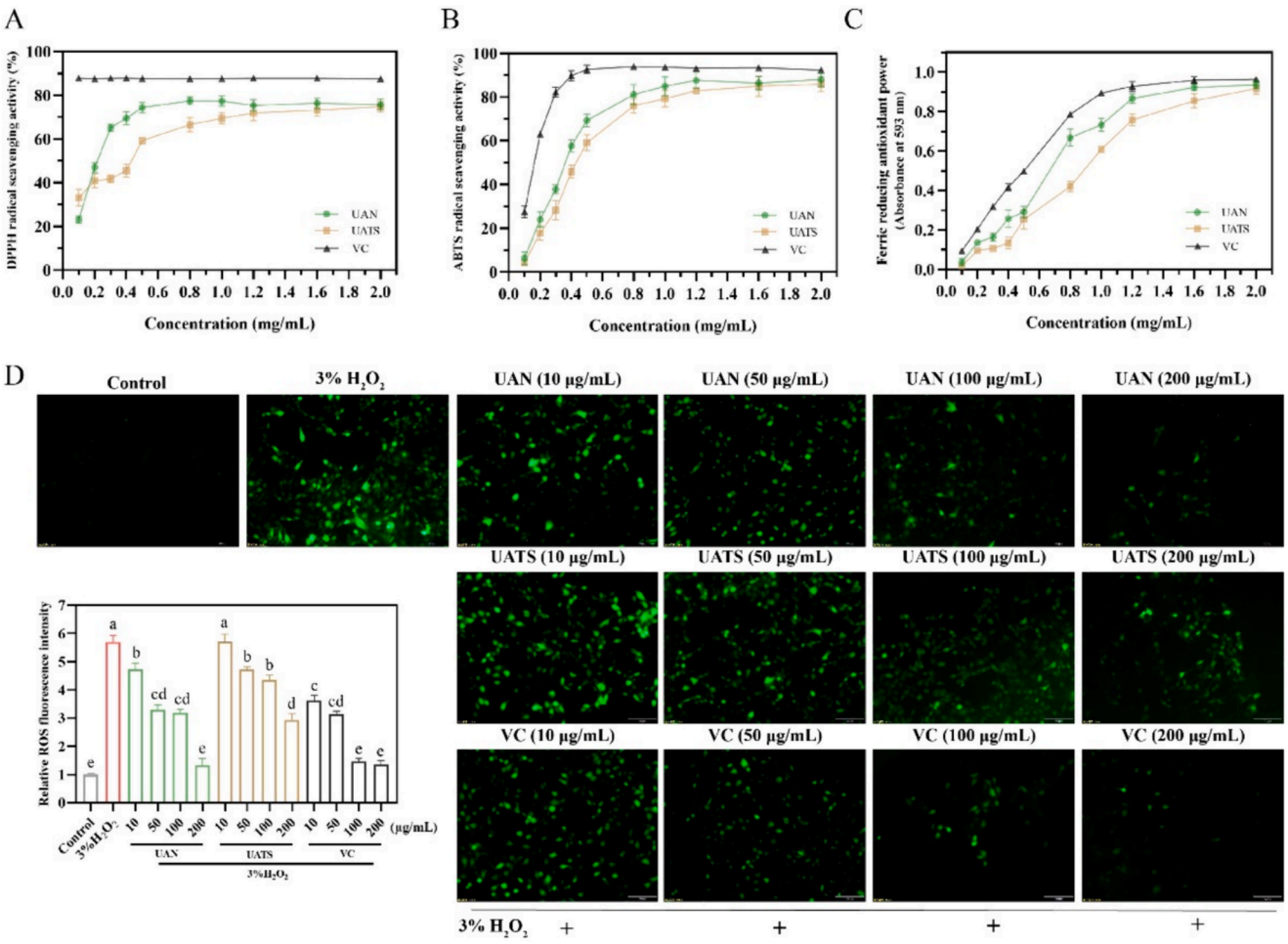


**Fig. 6.** Antioxidant activity of different concentrations of solution *in vitro*. (A) DPPH scavenging abilities. (B) $ABTS^{+}$ scavenging abilities. (C) Ferric reducing antioxidant power. (D) 3 % $H_2O_2$ induced oxidative damage of IPEC cells.

comprised of Bet-urea. Additionally, *in vitro* antioxidant assessments revealed that MOLF extracted by UAN displayed superior performance compared to that extracted by UATS, showcasing enhanced antioxidant efficacy. This study introduced a novel approach for the efficient extraction of bioactive compounds and substantiates its superior bioactive effects compared to conventional methods.

## CRediT authorship contribution statement

**Weilong Peng:** Funding acquisition, Formal analysis, Data curation, Conceptualization. **Xiaoguang Wang:** Writing – review & editing. **Weimei Wang:** Writing – review & editing. **Yaya Wang:** Writing – review & editing, Writing – original draft. **Junjie Huang:** Writing – review & editing. **Ruigang Zhou:** Writing – review & editing. **Ruonan Bo:** Writing – review & editing. **Mingjiang Liu:** Writing – review & editing. **Shaojie Yin:** Writing – review & editing, Conceptualization. **Jingui Li:** Writing – review & editing, Validation, Supervision, Funding acquisition, Formal analysis, Conceptualization.

## Declaration of competing interest

The authors declare that they have no known competing financial interests or personal relationships that could have appeared to influence the work reported in this paper.

## Acknowledgments

This work was supported in part by grants from the National Natural Science Foundation of China (32302920; 32072911); the Natural Science Foundation of Jiangsu Higher Education Institutions (22KJB230001) and the Priority Academic Program Development of Jiangsu Higher Education Institutions (PAPD).

## Appendix A. Supplementary data

Supplementary data to this article can be found online at https://doi.org/10.1016/j.ultsonch.2024.107003.

## References

[1] Y. Zhu, P. Du, J. Yang, Q. Yin, Y. Yang, Screening of multiclass pesticide residues in maca and Moringa oleifera by a modified QuEChERS sample preparation procedure and UPLC-ESI-MS/MS analysis. RSC Adv. 10, 36906–36919.
[2] A.A. Al-Ghanayem, M.S. Alhussaini, M. Asad, B. Joseph, Effect of Moringa oleifera leaf extract on excision wound infections in rats: antioxidant, antimicrobial, and gene expression analysis, Molecules 27 (2022) 4481.
[3] F. Gu, et al., Ultrasonic-cellulase synergistic extraction of crude polysaccharides from Moringa oleifera leaves and alleviation of insulin resistance in HepG2 cells, Int. J. Mol. Sci. 23 (2022) 12405.
[4] X. Jiang, et al., Moringa oleifera leaf improves meat quality by modulating intestinal microbes in white feather broilers, Food Chem. X 20 (2023).
[5] A.B. Falowo, et al., Multi-functional application of *Moringa oleifera* Lam. in nutrition and animal food products: A review, Food Res. Int. 106 (2018) 317–334.
[6] P. Chumark, et al., The *in vitro* and *ex vivo* antioxidant properties, hypolipidaemic and antiatherosclerotic activities of water extract of *Moringa oleifera* Lam. leaves, J. Ethnopharmacol. 116 (2008) 439–446.

[7] M. Lin, J. Zhang, X. Chen, Bioactive flavonoids in *Moringa oleifera* and their health-promoting properties, J. Funct. Foods 47 (2018) 469–479.
[8] K.M.M. John, et al., Metabolic variations, antioxidant potential, and antiviral activity of different extracts of Eugenia singampattiana (an Endangered Medicinal Plant Used by Kani Tribals, Tamil Nadu, India) Leaf, BioMed. Res. Int. 2014 (2014) 726145.
[9] M.S. Abdel-Kader, et al., Chemistry and biological activities of cannflavins of the cannabis plant, Cannabis Cannabinoid Res. 8 (2023) 974–985.
[10] E. El Maaiden, et al., Deep eutectic solvent-ultrasound assisted extraction as a green approach for enhanced extraction of naringenin from Searsia tripartita and retained their bioactivities, Front. Nutr. 10 (2023) 1193509.
[11] M. Tobiszewski, M. Marć, A. Gałuszka, J. Namieśnik, Green chemistry metrics with special reference to green analytical chemistry, Molecules 20 (2015) 10928–10946.
[12] C. Cannavacciuolo, et al., Natural Deep Eutectic Solvents (NADESs) combined with sustainable extraction techniques: A review of the green chemistry approach in food analysis, Foods Basel Switz. 12 (2022) 56.
[13] A. García-Roldán, L. Piriou, P. Jauregi, Natural deep eutectic solvents as a green extraction of polyphenols from spent coffee ground with enhanced bioactivities, Front. Plant Sci. 13 (2022) 1072592.
[14] C.B.T. Pal, G.C. Jadeja, Deep eutectic solvent-based extraction of polyphenolic antioxidants from onion (Allium cepa L.) peel, J. Sci. Food Agric. 99 (2019) 1969–1979.
[15] A.N. Syarifah, H. Suryadi, H. Hayun, A. Simamora, A. Mun'im, Detoxification of comfrey (Symphytum officinale L.) extract using natural deep eutectic solvent (NADES) and evaluation of its anti-inflammatory, antioxidant, and hepatoprotective properties, Front. Pharmacol. 14 (2023) 1012716.
[16] D.-T. Wu, et al., Ultrasound-assisted deep eutectic solvent extraction of phenolic compounds from thinned young kiwifruits and their beneficial effects, Antioxid. Basel Switz. 12 (2023) 1475.
[17] M.H. Shafie, D. Samsudin, R. Yusof, C.-Y. Gan, Characterization of bio-based plastic made from a mixture of Momordica charantia bioactive polysaccharide and choline chloride/glycerol based deep eutectic solvent, Int. J. Biol. Macromol. 118 (2018) 1183–1192.
[18] C. Wen, et al., Advances in ultrasound assisted extraction of bioactive compounds from cash crops – A review, Ultrason. Sonochem. 48 (2018) 538–549.
[19] I.M. Yusoff, Z. Mat Taher, Z. Rahmat, L.S. Chua, A review of ultrasound-assisted extraction for plant bioactive compounds: Phenolics, flavonoids, thymols, saponins and proteins, Food Res. Int. Ott. Ont 157 (2022) 111268.
[20] M. Menezes Maciel Bindes, M. Hespanhol Miranda Reis, V. Luiz Cardoso, D. C. Boffito, Ultrasound-assisted extraction of bioactive compounds from green tea leaves and clarification with natural coagulants (chitosan and Moringa oleífera seeds), Ultrason. Sonochem. 51 (2019) 111–119.
[21] L. Duan, L.-L. Dou, L. Guo, P. Li, E.-H. Liu, Comprehensive evaluation of deep eutectic solvents in extraction of bioactive natural products, ACS Sustain. Chem. Eng. 4 (2016) 2405–2411.
[22] X. Shang, D. Chu, J. Zhang, Y. Zheng, Y. Li, Microwave-assisted extraction, partial purification and biological activity in vitro of polysaccharides from bladder-wrack (Fucus vesiculosus) by using deep eutectic solvents, Sep. Purif. Technol. 259 (2021) 118169.
[23] P. Namazi, et al., Evaluation of functional groups of bioactive compounds, antioxidant potential, total phenolic and total flavonoid content of red bell pepper extracts, Food Sci. Technol. 18 (2021) 301–311.
[24] Z. Wang, S. Yang, Y. Gao, J. Huang, Extraction and purification of antioxidative flavonoids from Chionanthus retusa leaf, Front. Bioeng. Biotechnol. 10 (2022) 1085562.
[25] L. Wu, L. Li, S. Chen, L. Wang, X. Lin, Deep eutectic solvent-based ultrasonic-assisted extraction of phenolic compounds from *Moringa oleifera* L. leaves: Optimization, comparison and antioxidant activity, Sep. Purif. Technol. 247 (2020) 117014.
[26] S. Feng, et al., Extraction and identification of polyphenol from *Camellia oleifera* leaves using tailor-made deep eutectic solvents based on COSMO-RS design, Food Chem. 444 (2024) 138473.
[27] K. Li, et al., Green and efficient method to acquire high-value phycobiliprotein from microalgal biomass involving deep eutectic solvent-based ultrasound-assisted extraction, Food Chem. 449 (2024) 139196.
[28] Z. Fu, et al., Antioxidant activities and polyphenols of sweet potato (*Ipomoea batatas* L.) leaves extracted with solvents of various polarities, Food Biosci. 15 (2016) 11–18.
[29] C.-H. Liu, et al., Antioxidant triterpenoids from the stems of *Momordica charantia*, Food Chem. 118 (2010) 751–756.
[30] I. Fidrianny, H. Suhendy, M. Insanu, Correlation of phytochemical content with antioxidant potential of various sweet potato (Ipomoea batatas) in West Java, Indonesia, *Asian Pac. J. Trop. Biomed.* 8 (2018) 25.
[31] O. Zannou, I. Koca, T.M.S. Aldawoud, C.M. Galanakis, Recovery and stabilization of anthocyanins and phenolic antioxidants of roselle (Hibiscus sabdariffa L.) with hydrophilic deep eutectic solvents, Molecules 25 (2020) 3715.
[32] S.S. Patil, A. Pathak, V.K. Rathod, Optimization and kinetic study of ultrasound assisted deep eutectic solvent based extraction: A greener route for extraction of curcuminoids from Curcuma longa, Ultrason. Sonochem. 70 (2021) 105267.
[33] Y. Liu, et al., Ultrasonic-assisted extraction of polyphenolic compounds from Paederia scandens (Lour.) Merr. Using deep eutectic solvent: optimization, identification, and comparison with traditional methods, Ultrason. Sonochem. 86 (2022) 106005.
[34] K. Kumar, S. Srivastav, V.S. Sharanagat, Ultrasound assisted extraction (UAE) of bioactive compounds from fruit and vegetable processing by-products: A review, Ultrason. Sonochem. 70 (2021) 105325.
[35] Q. Zhang, K. De Oliveira Vigier, S. Royer, F. Jérôme, Deep eutectic solvents: syntheses, properties and applications, Chem. Soc. Rev. 41 (2012) 7108–7146.
[36] C. Fursenco, T. Calalb, L. Uncu, M. Dinu, R. Ancuceanu, Solidago virgaurea L.: A review of its ethnomedicinal uses, phytochemistry, and pharmacological activities, Biomolecules 10 (2020) 1619.
[37] Y. Wang, et al., Natural deep eutectic solvent-assisted extraction, structural characterization, and immunomodulatory activity of polysaccharides from Paecilomyces hepiali, Molecules 27 (2022) 8020.
[38] H. Qu, et al., An efficient approach for extraction of polysaccharide from abalone (Haliotis Discus Hannai Ino) viscera by natural deep eutectic solvent, Int. J. Biol. Macromol. 244 (2023) 125336.
[39] C. Liu, et al., Total biflavonoids extraction from Selaginella chaetoloma utilizing ultrasound-assisted deep eutectic solvent: Optimization of conditions, extraction mechanism, and biological activity in vitro, Ultrason. Sonochem. 98 (2023) 106491.
[40] S. Kilani, et al., Investigation of extracts from (Tunisian) Cyperus rotundus as antimutagens and radical scavengers, Environ. Toxicol. Pharmacol. 20 (2005) 478–484.
[41] H. Xue, et al., Ultrasound-assisted extraction of flavonoids from Potentilla fruticosa L. using natural deep eutectic solvents, *Molecules* 27 (2022) 5794.
[42] J. Liu, C. Li, G. Ding, W. Quan, Artificial intelligence assisted ultrasonic extraction of total flavonoids from Rosa sterilis, Mol. Basel Switz. 26 (2021) 3835.
[43] L.-L. Zheng, et al., Ultrasound-assisted extraction of total flavonoids from Aconitum gymnandrum, Pharmacogn. Mag. 10 (2014) S141.
[44] N.D. Oktaviyanti, et al., A green extraction design for enhancing flavonoid compounds from Ixora javanica flowers using a deep eutectic solvent, R. Soc. Open Sci. 7 (2020) 201116.
[45] L. Zhang, M. Wang, Optimization of deep eutectic solvent-based ultrasound-assisted extraction of polysaccharides from Dioscorea opposita Thunb, Int. J. Biol. Macromol. 95 (2017) 675–681.
[46] S. Sreekumar, F.M. Goycoolea, B.M. Moerschbacher, G.R. Rivera-Rodriguez, Parameters influencing the size of chitosan-TPP nano- and microparticles, Sci. Rep. 8 (2018) 4695.
[47] Z. Li, Q. Li, Ultrasonic-assisted efficient extraction of coumarins from Peucedanum decursivum (Miq.) maxim using deep eutectic solvents combined with an enzyme pretreatment, Molecules 27 (2022) 5715.
[48] Ultrasound assisted extraction of food and natural products, Mechanisms, techniques, combinations, protocols and applications. A review, *Ultrason. Sonochem.* 34 (2017) 540–560.
[49] J. Zhang, C. Wang, Q. Li, W. Liang, Polysaccharides from radix peucedani: extraction, structural characterization and antioxidant activity, Molecules 28 (2023) 7845.
[50] J. Zhou, et al., LC-MS-based metabolomics reveals the chemical changes of polyphenols during high-temperature roasting of large-leaf yellow tea, J. Agric. Food Chem. 67 (2019) 5405–5412.
[51] S. Chigurupati, et al., Molecular docking of phenolic compounds and screening of antioxidant and antidiabetic potential of Moringa oleifera ethanolic leaves extract from Qassim region, Saudi Arabia, *Saudi J. Biol. Sci.* 29 (2022) 854–859.
[52] S. Tshepelevitsh, K. Hernits, I. Leito, Prediction of partition and distribution coefficients in various solvent pairs with COSMO-RS, J. Comput. Aided Mol. Des. 32 (2018) 711–722.
[53] M. Lazović, et al., Efficiency of natural deep eutectic solvents to extract phenolic compounds from agrimonia eupatoria: experimental study and in silico modelling, Plants 11 (2022) 2346.
[54] J. AlYammahi, et al., Natural deep eutectic solvents for ultrasonic-assisted extraction of nutritious date sugar: molecular screening, experimental, and prediction, Ultrason. Sonochem. 98 (2023) 106514.
[55] F. Alshammari, M.B. Alam, B.-R. Song, S.-H. Lee, Antioxidant, tyrosinase, α-glucosidase, and elastase enzyme inhibition activities of optimized unripe Ajwa Date Pulp (Phoenix dactylifera) extracts by response surface methodology, Int. J. Mol. Sci. 24 (2023) 3396.
[56] K.-L. Cheong, J.-K. Li, S. Zhong, Preparation and structure characterization of high-value laminaria digitata oligosaccharides, Front. Nutr. 9 (2022) 945804.
[57] K. Szentmihályi, K. Süle, A. Egresi, A. Blázovics, Z. May, Metronidazole does not show direct antioxidant activity in in vitro global systems, Heliyon 7 (2021).